



Simulation in Metallurgical Processing: Recent Developments and Future Perspectives

ANDREAS LUDWIG,^{1,3,4} MENGHUAI WU,² and ABDELLAH KHARICHA¹

1.—Department of Metallurgy, Montanuniversitaet Leoben, Leoben, Austria. 2.—Christian-Doppler Laboratory for Advanced Process Simulation of Solidification and Melting, Department Metallurgy, Montanuniversitaet Leoben, Leoben, Austria. 3.—e-mail: ludwig@unileoben.ac.at. 4.—e-mail: smmp@unileoben.ac.at

This article briefly addresses the most important topics concerning numerical simulation of metallurgical processes, namely, multiphase issues (particle and bubble motion and flotation/sedimentation of equiaxed crystals during solidification), multiphysics issues (electromagnetic stirring, electro-slag remelting, Cu-electro-refining, fluid–structure interaction, and mushy zone deformation), process simulations on graphical processing units, integrated computational materials engineering, and automatic optimization via simulation. The present state-of-the-art as well as requirements for future developments are presented and briefly discussed.

INTRODUCTION

Numerical process simulations are nowadays standard for designing and optimization of metallurgical processes.¹ Furnace construction, tundish planning, or designing of continuous casting machines are assisted by the beforehand use of simulation tools. On the other hand, many metallurgical processes need multiphase and/or multiphysics descriptions to account for essential process details; yet, often these descriptions are missing or only roughly available. In this article, which is based on two former review reports by the same authors,^{2,3} a short overview on present developments and future directions in the field is provided.

MULTIPHASE SIMULATION

Motion of Particles/Bubbles

Understanding the behavior of nonmetallic inclusions (particles) or gas bubbles in molten steel is an important topic in primary and secondary metallurgy.⁴ Examples are the gas bubble flow in steel-making vessels, melt stirring in ladles to maintain thermal homogeneity and reduce nonmetallic inclusions, melt flow and removal of nonmetallic inclusions in tundishes, blowing argon gas into submerged entry nozzle (SEN) during continuous casting to minimize the risk of clogging, etc. The most common way of modeling the motion of bubbles/particles in

molten steel is the usage of the so-called disperse phase method (DPM). The turbulent flow of the molten steel can be obtained by solving the Navier–Stokes equation together with corresponding turbulence equations, while the trajectory of particles/bubbles (or packets of particles/bubbles) are calculated by solving Newton's law for the motion of bubbles/particles considering their interaction with the turbulent melt flow.^{5–8} The impact of bubbles on the transient, turbulent flow in a continuous caster for steel slabs⁸ and bubble coagulation and breakup were also investigated by using this approach.⁹ Recently, the current authors performed laboratory water-particle flow experiments to evaluate such a DPM model and discussed remarkable agreement between experiments and simulations.¹⁰

Flotation/Sedimentation of Equiaxed Crystals During Solidification

In practical casting processes, equiaxed crystals forming during solidification can move freely, either float or sediment, to form the as-cast structure. This kind of motion of crystals can cause significant structural and compositional heterogeneity, i.e., macrosegregation. To model the nucleation, growth, motion, and sedimentation of equiaxed crystals, a multiphase volume-average approach was proposed.^{11,12} Different from the aforementioned DPM method, the equiaxed crystals are here treated as a

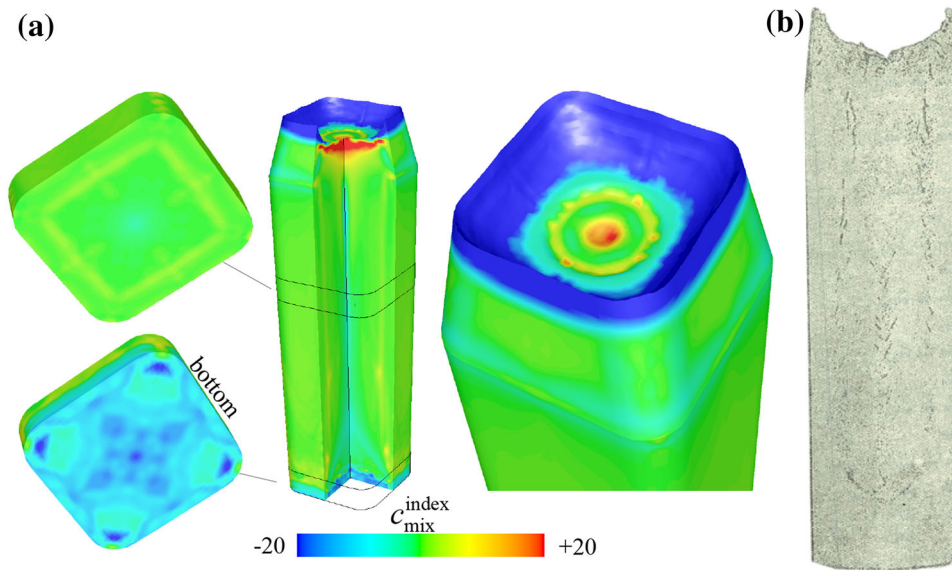


Fig. 1. A four-phase model is used to simulate macrosegregation and shrinkage cavity in a 2.45-ton, industry-scale steel ingot. (a) The predicted macrosegregation, i.e., contour of the index of the mixture concentration of carbon, is compared with (b) real casting trial, i.e., sulfur print of the vertical section. A corresponding model description can be found in the original literature. Figures reprinted with permission from Ref. 32.

pseudo-liquid phase (secondary fluid phase), interpenetrating and incorporating with the parent melt (primary fluid phase). The number density, grain size, moving velocity, and other physical quantities of equiaxed phases are volume-averaged and calculated by solving an additional set of conservation equations. Mass transfer due to solidification, momentum, and energy transfer between the parent melt and the growing and moving equiaxed crystals are considered in closure laws. Herein, the equation of motion of equiaxed grains is solved by using an effective viscosity for the solid/liquid mixture. This approach was used to model pure equiaxed solidification,^{13–18} mixed columnar-equiaxed solidification^{19–26} (with predictions on Columnar-to-Equiaxed Transition (CET)), equiaxed solidification with dendritic morphology,^{27,28} and mixed columnar-equiaxed solidification with dendritic morphology.^{26,29–31} Recently, a four-phase solidification model, i.e., combining the three-phase mixed columnar-equiaxed solidification with the description of shrinkage cavity, is used to calculate the formation of macrosegregation and shrinkage cavity in a 2.45-ton steel ingot (Fig. 1).³²

MULTIPHYSICS SIMULATION

Electromagnetic Stirring

The ability of electromagnetic stirring a melt during solidification to improve the final material quality has been long recognized. The most important benefit of electromagnetic stirring a melt is its ability to enhance the transition from columnar to equiaxed solidification. Other advantages are the homogenization of the liquid metal flow, the reduction of surface or subsurface defects, as well as the

reduction of center segregation. Due to the complexity of metallurgical processes, it is difficult to access and measure the flow of molten metals.³³ Simulation of the magnetohydrodynamic (MHD) flow is at the moment the only way to estimate the phenomena occurring during electromagnetic stirring. In some early work, Spitzer³⁴ discovered the existence of a secondary flow, aside from the primary rotating stirring flow, by using numerical simulations. These predictions were validated with experimental observations. In recent years, more international research has been conducted by using numerical simulation and experimental studies.^{35–39} Nevertheless, this research has focused mainly on the magnetohydrodynamic flow field, and even though it has investigated the temperature field distribution under electromagnetic stirring, it has not considered the interaction with solidification. At the present stage, most of the studies are performed experimentally, but large scientific efforts are still necessary to build a model able to couple MHD, CET, and formation of segregation during solidification.

Electro-Slag Remelting

Nowadays, the demand for very large heavy ingots (>100 tons) through the electro-slag remelting (ESR) process is increased, especially in the chemical, oil, and gas industries. The multiphysics of the ESR process involves melting, solidification, heat transfer, mass transfer, and MHD. Nearly all proposed CFD models for ESR are in two dimensions (2D). There are only a very small number of three-dimensional (3D) calculations. The limitations of computational resources are constraining researchers to perform full-scale 3D simulations.

One example presented by Kharicha et al.⁴⁰ modeled the effects of the slag-pool interface movement, formation, departure, and dripping of droplets through the slag for an industrial-scale (ϕ 600 mm ingot) ESR process. The interaction between flow and electromagnetic field was found to generate a strong 3D flow, which could not be predicted by typical 2D models. Recently, Wang et al.⁴¹ established a 3D model to investigate a laboratory-scale ESR process (ϕ 120 mm ingot). The multiphase volume of fluid (VOF) approach was used to model the melting of electrodes with the formation of droplets as well as slag pool interface movement. Karimi-Sibaki et al.⁴² performed a full 3D simulation of an industrial-scale, electro-slag remelting process as well as 2D calculations under the same conditions. Both the 2D and 3D conditions assume an implicit modeling of the falling droplet and neglect slag/pool interface oscillations. The electromagnetic field, its interaction with the turbulent flow in the molten slag and melt pool regions, the thermal field of the entire ESR system (including electrode, molten slag, ingot, and mold), and the solidification of the ingot were calculated. Nonaxis symmetry flow pattern and temperature field in the slag region were predicted, which are very similar to those experimentally observed in situ from the exposed slag surface during operation. Statistics of the turbulent flow in the slag and melt pool were performed to characterize quantitatively the transient behavior of the flow. The mean velocity and temperature fields averaged over 30 min are illustrated in Fig. 2. By comparing the 3D calculation with a 2D axis-symmetrical calculation, it is found that the predicted melt pool profiles are similar,

leading to the conclusion that, at conventional scale, a 2D calculation is sufficient for the prediction of the melt pool profile. In other words, the fast transient 3D flow in the slag region has only a limited influence on the ingot solidification characteristics.

Cu Electro-Refining

The copper refining electrolysis process is essential for producing high-purity copper at an industrial scale. The challenge for a corresponding numerical process simulation is that the driving phenomena for natural convection (dissolution and plating of copper) happens in the 100- μm vicinity of the electrodes, whereas force convection is governed by in- and outlets of the full tankhouse cell, which is in the order of several meters. Hence, simultaneous calculation of natural and forced convection in a full-scale tankhouse cell is at present impractical if not impossible. The number of cells would be far too large. Therefore, in Ref. 43 it was suggested to break down the simulation into two parts. First, the natural convection caused by the density changes of the electrolyte is simulated in a “local” simulation covering one anode–cathode pair. Second, the flow of the electrolyte caused by the forced convection is simulated at a “global” scale, whereby the results from the “local” simulation are included by individual in-/outlet surfaces in between the multiple anode–cathode gaps. With that approach, it was possible to identify areas with insufficient electrolyte movement in a full-scale copper refining electrolysis cell. With this information, an improper concentration of inhibitors and/or undesired anode slimes occurrence can numerically be detected.

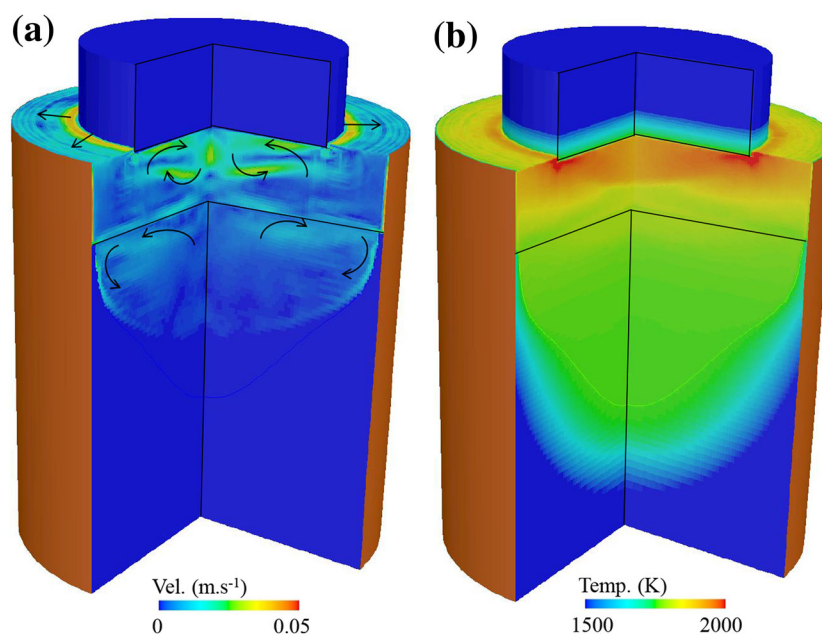


Fig. 2. Mean velocity field (a) and mean temperature field (b) averaged over a time period of 1800 s for an industrial-scale ESR process. Figures reprinted with permission from Ref. 42.

Fluid–Structure Interaction

Solidification involves both fluid dynamic and structure mechanical issues. The classic term of fluid–structure interaction is mostly used for problems where a fluid and a solid body exchange momentum by the deformation of a predefined interface. Describing the fluid flow is a typical computational fluid dynamics (CFD) problem, whereas describing the deformation of the solid domain is a typical finite element method (FEM) problem. The interplay of CFD and FEM happens via the interface between the fluid and mechanical domains. The state-of-the-art solution to this issue is to couple both CFD-based and FEM-based codes by considering data transfer at the domain interface.^{44,45} Of course, the two domains must be remeshed consistently. Unfortunately, this solution cannot be used directly for the solidification because the interface between the fluid domain (liquid melt) and the mechanical domain (solidified region including mushy zone) is not pre-describable. A monolithic formulation treating the fluid–structure interaction sounds like a better alternative,⁴⁶ but it is still not applicable for solidification as the difference between liquid viscosity and the solid consistency is huge. Therefore, Bellet et al. suggested a partitioned formulation to treat this issue⁴⁷ with the solidifying mushy zone as part of the solution. This partitioned formulation has been used to calculate

the solidification of an ingot casting with the consideration of the deforming solid shell. This topic is still in its infant stage, and it is subject to further development.

Mushy Zone Deformation

During solidification of castings, equiaxed crystals having formed sink downward, sediment, and form a packed bed. The behavior of separated moving crystals can be described by a submerged object approach, whereas the viscoplastic behavior of a semisolid slurry follows a volume-averaged viscoplastic constitutive equation. In Refs. 48 and 49, a two-phase Eulerian–Eulerian volume-averaging approach is used to combine both flow regimes. The transition happens at a certain solid volume fraction, the so-called coherency limit. Starting with a uniform distribution of crystals in rest, sedimentation and packing of crystals are described together with deformation of and stress evolution in the backed bed. It is shown that semisolid channels where liquid can flow more easily might exist in between the coherent solid areas (Fig. 3) and that the formation of a continuous crystal pileup and a corresponding initiation of a crystal avalanche/collapsing can be predicted. The model is the first step toward describing the formation of the solidifying shell together with the occurring gap between mold and metal during thin slab casting of steel.

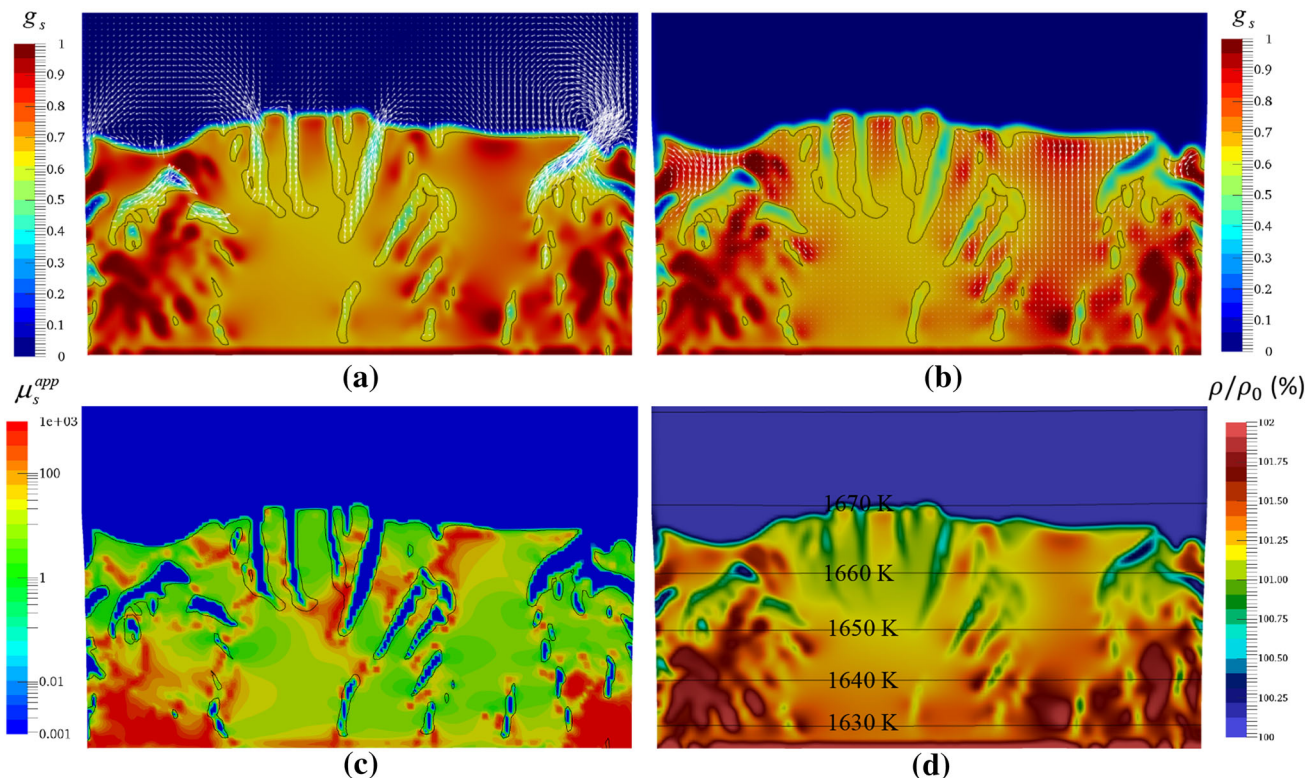


Fig. 3. Modeling example of solid packing and liquid draining during sedimentation of equiaxed crystals. (a) and (b) show solid fraction with liquid and solid velocity vectors; (c) apparent kinematic viscosity of the solid distribution; and (d) relative density distribution. Figures reprinted with permission from Ref. 48.

PROCESS SIMULATIONS ON GPUS

Scientific calculations on modern graphic cards, so-called graphical processing units (GPUs), have the potential of being a factor of 10–100 times faster than the classic methods using central processing units (CPUs).^{50–52} Nevertheless, to achieve such huge accelerations, the numerical approach must take full advantage of the GPU architecture. The smoothed-particle hydrodynamics (SPH) technique has been established as one of the major concepts for fluid animation in computer graphics.⁵³ Nowadays, complex scenes with millions of sampling points, one- and two-way coupled rigid and elastic solids, multiple phases, and additional features such as foam or air bubbles can be computed at reasonable expense. Yet, the technique still needs some major developments to transform from being a computer graphics tool into a tool for solving scientific problems. Principally, the simplicity offered by this method made some complex system in physics such as fluid–structure interaction, free interface, and properties jumping with multiple material boundaries become relatively easy to simulate. Nevertheless, solidification and melting have been simulated with SPH mainly for computer graphics purposes, and scientific and accurate simulations are sparse. The present authors have developed a code intending to demonstrate the possibility of simulating heat-driven flows encountered in various problems in the metallurgical industry.⁵⁴ The ultimate aim is to carry out such simulations for the metallurgical industry where large temperature differences exist in space and time. We have especially studied the buoyancy-driven flow, Boussinesq and non-Boussinesq, with the SPH method. Specifically a semi-implicit version of SPH has been modified for these two kinds of flows. Figure 4 shows the results of the solidification after the casting of an aluminum alloy. The numerical and experimental results can be compared in terms of the shrinkage cavity. At present, this group of authors is further developing the method to model phenomena occurring in continuous casting, such as turbulence and electromagnetic stirring.

INTEGRATED COMPUTATIONAL MATERIALS ENGINEERING

Integrated computational materials engineering (ICME), i.e., using the computational approach to design engineering products by linking different materials modeling tools at multiple length scales, addresses the importance of information exchange between the heterogeneous varieties of numerous simulation tools. This strategy has recently been promoted by the US government via the Materials Genome Initiative* and the EU-commission via the Integrated Computational Materials Engineering

*<https://www.whitehouse.gov/mgi>.

**<http://web.micress.de/ICMEg1/>.

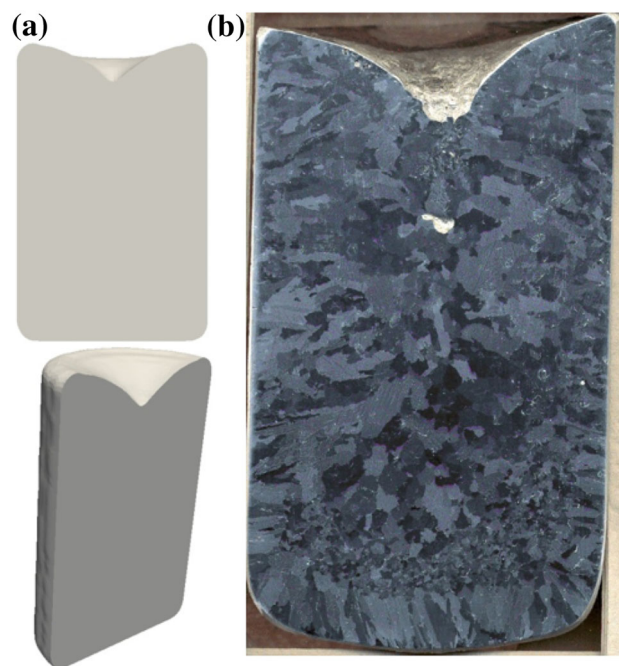


Fig. 4. Modeling of solidification including the formation of a shrinkage pipe modeled with an improved SPH approach using 60,000 particles (a). The laboratory Al-Cu ingot has a diameter of 75 mm (b).

expert group.** The challenge for solidification scientists and metallurgists is twofold. Reliable models for prediction of an as-cast microstructure, including casting defects under the production conditions, are required on the one hand, and common database/data-structure shared with and flexible data flow interface to other materials processing tools within the production chain must be created on the other hand. Preliminarily, some trial modeling examples following this strategy can be found in Refs. 55–58. The earlier approach, called through-process modeling,^{56,57} belongs to the ICME as well.

AUTOMATIC PROCESS OPTIMIZATION VIA SIMULATIONS

Automatic process optimization via simulations (APOS) is a technique for optimization of the materials processing parameters by performing process simulations automatically. A target function that characterizes the product quality, and/or the production cost/time, must be defined. Following some optimization algorithms, e.g., gradient method and evolution strategy,⁵⁹ repeated process simulations will be run by adjusting the processing parameters automatically until the target product quality and cost are achieved. One demonstrative example⁶⁰ is presented to show how APOS is applied to optimize the local heat treatment parameters to achieve the target mechanical property. The mechanic properties of many aluminum alloys can be changed by a heat treatment and quenching

procedure. If locally a strengthening of the alloy is needed, a localized heat treatment and quenching procedure may be an alternative to the energy-intensive and costly treatment of the whole part. Nevertheless, it is not clear which process parameters are required to achieve the desired local strengthening. Therefore, the optimization scheme performs a series of process simulations where LASER power, beam diameter, and exposure time are varied automatically until the energy minimized process is found that ensures sufficient local strengthening of the alloy.

CONCLUSION AND SUMMARY

Process simulations for metallurgical processes have become a daily routine for engineers working in industry. Yet, many processes are multiphase and multiphysics in nature. Considering corresponding phenomena in detail is soon bringing the standard simulation tools to the edge of their ability. In the next decades, the following is greatly needed: (I) new, more sophisticated model considerations; (II) new/improved software strategies that might save most of the computation efforts; and (III) companies willing to take the effort to verify numerical predictions by measuring process details even during their production.

ACKNOWLEDGEMENTS

Open access funding provided by Montanuniversität Leoben. The authors are grateful for financial support from RHI Technologies, INTECO special melting technologies GmbH, Atlantic Copper, Aurubis AG, Aurubis Belgium, Boliden Mineral, Kennecott Utah Copper, Montanwerke Brixlegg, and Outotec Finland. Also, part of this work was financial supported by the Christian-Doppler Society and the Austrian Federal Government (in particular by the Bundesministerium für Verkehr, Innovation und Technologie, and the Bundesministerium für Wirtschaft, Familie und Jugend) and the Styrian Provincial Governments, represented by Österreichische Forschungsförderungsgesellschaft mbH and by Steirische Wirtschaftsförderungsgesellschaft mbH, within the research activities of the K2 Competence Centre on “Integrated Research in Materials, Processing and Product Engineering,” operated by the Materials Center Leoben Forschung GmbH in the framework of the Austrian COMET Competence Centre Programme, for which the authors are grateful.

OPEN ACCESS

This article is distributed under the terms of the Creative Commons Attribution 4.0 International License (<http://creativecommons.org/licenses/by/4.0/>), which permits unrestricted use, distribution, and reproduction in any medium, provided you give appropriate credit to the original author(s) and the

source, provide a link to the Creative Commons license, and indicate if changes were made.

REFERENCES

1. M. Rappaz, M. Bellet, and M. Deville, *Numerical Modelling in Materials Science and Engineering* (New York: Springer, 1998).
2. A. Ludwig, A. Kharicha, and M. Wu, *Metall. Mater. Trans. B* 45, 36 (2013).
3. A. Ludwig, M. Wu, A. Kharicha, A. Vakhrushev, J. Bohacek, A. Kemminger, and E. Karimi-Sibaki, *BHM Berg Huettenmaenn. Monatsh.* 158, 184 (2013).
4. R.I.L. Guthrie, *Metall. Mater. Trans. B* 35, 417 (2004).
5. C. Pfeiler, M. Wu, and A. Ludwig, *Mater. Sci. Eng., A* 413–414, 115 (2005).
6. C. Pfeiler, M. Wu, A. Ludwig, C. Chimani, and J. Watzinger, *6th International Conference Model. Cast. Weld. Adv. Solidif. Process. (MCWASP VI)*, eds. C.-A. Gandin and M. Bellet (Opio; TMS Publication, 2006).
7. C. Pfeiler, B.G.G. Thomas, M. Wu, A. Ludwig, and A. Kharicha, *Steel Res. Int.* 79, 599 (2008).
8. Z.Q.Q. Liu, B.K.K. Li, and M.F.F. Jiang, *Metall. Mater. Trans. B* 45, 675 (2013).
9. T. Zhang, Z.G. Luo, C.L. Liu, H. Zhou, and Z.S. Zou, *Powder Technol.* 273, 154 (2015).
10. A. Vakhrushev, M. Wu, A. Ludwig, G. Nitzl, Y. Tang, and G. Hackl, *5th International Conference Simul. Model. Met. Process. Steelmak. (STEELSIM 2013)* (Ostrova, Czech Republic, 2013).
11. J. Ni and C. Beckermann, *Metall. Trans. B* 22, 349 (1991).
12. C. Beckermann and R. Viskanta, *Appl. Mech. Rev.* 46, 1 (1993).
13. A. Ludwig and M. Wu, *Metall. Mater. Trans. A* 33, 3673 (2002).
14. M. Wu, A. Ludwig, A. Bührig-Polaczek, M. Fehlbier, and P.R. Sahm, *Int. J. Heat Mass Transf.* 46, 2819 (2003).
15. M. Wu and A. Ludwig, *Mater. Sci. Eng. A* 413–414, 192 (2005).
16. M. Wu, A. Ludwig, and J. Luo, *Mater. Sci. Forum* 475–479, 2725 (2005).
17. M. Wu, A. Ludwig, and L. Ratke, *Model. Simul. Mater.* 0393, 755 (2003).
18. T.M. Wang, S. Yao, X.G. Zhang, J.Z. Jin, M. Wu, A. Ludwig, B. Pustal, and A. Bührig-Polaczek, *Acta Metall. Sin.* 42, 584 (2006).
19. A. Ludwig and M. Wu, *Mater. Sci. Eng. A* 413–414, 109 (2005).
20. A. Ludwig, M. Gruber-Pretzler, F. Mayer, A. Ishmurzin, and M. Wu, *Mater. Sci. Eng. A* 413–414, 485 (2005).
21. M. Wu and A. Ludwig, *Metall. Mater. Trans. A* 37, 1613 (2006).
22. M. Wu and A. Ludwig, *Metall. Mater. Trans. A* 38, 1465 (2007).
23. M. Wu, L. Könözy, A. Ludwig, W. Schützenhöfer, and R. Tanzer, *Steel Res. Int.* 79, 637 (2008).
24. M. Wu, J. Li, A. Ludwig, and A. Kharicha, *Comp. Mater. Sci.* 79, 830 (2013).
25. M. Wu, J. Li, A. Ludwig, and A. Kharicha, *Comp. Mater. Sci.* 92, 267 (2014).
26. M. Ahmadein, M. Wu, and A. Ludwig, *J. Cryst. Growth* 417, 65 (2015).
27. M. Wu and A. Ludwig, *Acta Mater.* 57, 5621 (2009).
28. M. Wu and A. Ludwig, *Acta Mater.* 57, 5632 (2009).
29. M. Wu, A. Fjeld, and A. Ludwig, *Comp. Mater. Sci.* 50, 32 (2010).
30. M. Wu, A. Ludwig, and A. Fjeld, *Comp. Mater. Sci.* 50, 43 (2010).
31. M. Ahmadein, M. Wu, J.H.H. Li, P. Schumacher, and A. Ludwig, *Metall. Mater. Trans. A* 44, 2895 (2013).
32. M. Wu, A. Kharicha, A. Ludwig, and I.O.P. Conf, *Ser. Mater. Sci. Eng.* 84, 012006 (2015).
33. F. Stefani, T. Gundrum, and G. Gerbeth, *Phys. Rev. E* 70, 056306 (2004).
34. K.H. Spitzer, M. Dubke, and K. Schwerdtfeger, *Metall. Trans. B* 17, 119 (1986).

35. K. Okazawa, T. Toh, J. Fukuda, T. Kawase, and M. Toki, *ISIJ Int.* 41, 851 (2001).
36. L.B. Trindade, A.C. Vilela, M.T. Vilhena, and R.B. Soares, *IEEE Trans. Magn.* 38, 3658 (2002).
37. F.C. Chang, J.R. Hull, and L. Beitelman, *Metall. Mater. Trans. B* 35, 1129 (2004).
38. M. Barna, B. Willers, J. Reiter, and S. Eckert, *2nd METEC ESTAD Conference* (2015), pp. 6–2015.
39. M. Javurek, M. Barna, P. Gittler, K. Rockenschaub, and M. Lechner, *Steel Res. Int.* 79, 617 (2008).
40. A. Kharicha, A. Ludwig, and M. Wu, *8th International Pamir Conference Fund. Appl. MHD* (Borgo France, 2011), pp. 695–699.
41. Q. Wang, Z. He, B. Li, and F. Tsukihashi, *Metall. Mater. Trans. B* 45, 2425 (2014).
42. E. Karimi-Sibaki, A. Kharicha, J. Bohacek, M. Wu, and A. Ludwig, *Adv. Eng. Mater.* 18, 224 (2015).
43. A. Kemminger and A. Ludwig, *Eur. Metall. Conf.* (Weimar, Germany, 2013), pp. 795–805.
44. H. Jasak and Z. Tukovic, *Eur. Conf. Comput. Fluid Dyn.* 1 (2010).
45. G. Papadakis, *J. Comp. Phys.* 227, 3383 (2008).
46. B. Hubner, E. Walhorn, and D. Dinkler, *Comput. Methods Appl. Mech. Eng.* 193, 2087 (2004).
47. O. Boughanmi and M. Bellet, *Steelsim* 2011, 1–10 (2011).
48. A. Ludwig, A. Vakhrushev, T. Holzmann, M. Wu, and A. Kharicha, *I.O.P. Conf. Ser. Mater. Sci. Eng.* 84, 012102 (2015).
49. A. Ludwig, A. Vakhrushev, M. Wu, T. Holzmann, and A. Kharicha, *Trans. Indian Inst. Metall.* 68, 1087 (2015).
50. E. Elsen, P. LeGresley, and E. Darve, *J. Comput. Phys.* 227, 10148 (2008).
51. D. Göddeke, S.H.M. Buijssen, H. Wobker, and S. Turek, *High Perform. Comput. Simul.*, eds. W.W. Smari and J. McIntire (2009), pp. 12–21.
52. A. Klöckner, T. Warburton, J. Bridge, and J.S. Hesthaven, *J. Comp. Phys.* 228, 7863 (2009).
53. M. Ihmsen, J. Orthmann, B. Solenthaler, A. Kolb, and M. Teschner, *Eurographics* 2014, 21 (2014).
54. A. Kharicha, S. Baig, M. Wu, and A. Ludwig, To be publ.
55. A. Ludwig, G. Unterreiter, M. Wu, B. Stauder, R. Tatschl, W. Edelbauer, R. Kopun, B. Basara, D. Zhang, C. Sommitsch, and F. Krumphals, *1st Int. Work. Softw. Solut. Integr. Comp. Mater. Eng.* (2014), p. 82.
56. P. Li, D.M.M. Maijer, T.C.C. Lindley, and P.D.D. Lee, *Mater. Sci. Eng. A* 460–461, 20 (2007).
57. D.M. Maijer, Y.X. Gao, P.D. Lee, T.C. Lindley, and T. Fukui, *Metall. Mater. Trans. A* 35, 3275 (2004).
58. M.C. Schneider, J.C. Sturm, W. Schaefer, E. Hepp, and V. Gurevich, *I.O.P. Conf. Ser. Mater. Sci. Eng.* 84, 012035 (2015).
59. N. Hofmann, S. Oliver, G. Laschet, F. Hediger, J. Wolf, and P.R. Sahn, *Model. Simul. Mater. Eng.* 5, 23 (1997).
60. T. Holzmann and A. Ludwig, *IOP Conf. Ser. Mater. Sci. Eng.* 119, 0120 (2016).